Eur. Phys. J. C (2022) 82:806
https://doi.org/10.1140/epjc/s10052-022-10737-8

THE EUROPEAN PHYSICAL JOURNAL C

Regular Article - Theoretical Physics

Gaussian discriminators between ΛCDM and wCDM cosmologies using expansion data

Ahmad Mehrabi[1,a], **Jackson Levi Said**[2,3,b]

[1] Department of Physics, Bu-Ali Sina University, Hamedan 65178, 016016, Iran
[2] Institute of Space Sciences and Astronomy, University of Malta, Msida, Malta
[3] Department of Physics, University of Malta, Msida, Malta

Received: 20 May 2022 / Accepted: 22 August 2022 / Published online: 9 September 2022

Abstract The Gaussian linear model provides a unique way to obtain the posterior probability distribution as well as the Bayesian evidence analytically. Considering the expansion rate data, the Gaussian linear model can be applied for ΛCDM, wCDM and a non-flat ΛCDM. In this paper, we simulate the expansion data with various precision and obtain the Bayesian evidence, then it has been used to discriminate the models. The data uncertainty is in range $\sigma \in (0.5, 10)\%$ and two different sampling rates have been considered. Our results indicate that considering $\sigma = 0.5\%$ uncertainty, it is possible to discriminate 2% deviation in equation of state from $w = -1$. On the other hand, we investigate how precision of the expansion rate data affects discriminating the ΛCDM from a non-flat ΛCDM model. Finally, we perform a parameters inference in both the MCMC and Gaussian linear model, using current available expansion rate data and compare the results.

1 Introduction

ΛCDM cosmology offers a simple and consistent concordance model which has agreed with observations for several decades [1,2]. Separately, the ΛCDM model gives excellent agreement with cosmic microwave background data [3,4], as well as late time measurements of cosmic expansion [5]. However, recent observations have suggested a growing cosmic tension in the reporting of the Hubble constant [6–8], among other tensions. Together with the long standing consistency issues with the model [9], this points to possible deviations from ΛCDM cosmology entering the observational regime. In this new context, it is imperative to understand the accuracy of observational data needed to discriminate between viable alternatives.

Cosmological tensions in the ΛCDM model has led to a re-evaluation of the foundations of the model such as the role of the cosmological principle [10,11], as well as the nature of dark matter and dark energy (such as Refs. [12–15]), and the fundamental description of gravity [16–20]. One such alternative that has gained popularity in recent years is the wCDM model. This is composed of a dynamical equation of state for dark energy that varies across the cosmic history of the Universe. It remains an open question whether observational constraints can point to a varying equation of state in the near future. Thus, it is important to understand what precision would be needed to discriminate between these two models.

Among all tensions and issues in the ΛCDM, the so called H_0 tension, is the most severe one. A Lot of efforts have been undertaken so far to tackle the problem without any reliable and satisfactory solution (to see more details refer to [21]). Notice that, along with all model modifications scenarios that have been considered so far, describing a data set in a model independent approach might be very useful in this case [22–24].

For a typical cosmological setup, one naturally investigates a Markov chain Monte Carlo (MCMC) approach to infer parameter values using the latest observational data sets (see [25] for a comprehensive review). However, given the plethora of cosmological models being proposed, this approach only gives the constrain on the free parameters and says nothing about model comparison. For this purpose, some statistical measures, under some simplifying assumptions, including the Akaike information criterion (AIC), the Bayesian information criterion (BIC) and Deviance information criterion (DIC) have been used for model selection. On the other hand the Bayesian evidence provides a robust and

[a] e-mail: Mehrabi@ipm.ir (corresponding author)
[b] e-mail: jackson.said@um.edu.mt

reliable measure for model selection. Unfortunately, computation of the quantity involves a high-dimension integration over the product of likelihood and prior, which is computationally very expensive. To overcome this, some numerical approaches like the nested sampling [26–28] and the Savage-Dickey density ratio [29] have been developed. However, when the model is linear in its free parameters, the Gaussian linear model (GLM) provides an analytic solution for the Bayesian evidence. The formalism for a Gaussian or flat prior has been presented in [30]. Moreover, the Bayesian model selection has been utilized in [31,32] to understand reliability of the Bayesian evidence. In this work, we consider three important cosmological models which are linear in their parameters and apply the GLM method to understand how precision of the expansion rate data affects the significance of the model discrimination through Bayesian evidence.

The structure of this paper is as follows: In Sect. 2, we give the basic formalism of the Gaussian linear model (GLM) and introduce the analytic formula to obtain the posterior distribution as well as the evidence. In Sect. 3, the details of simulated data in our models are given. In addition, we present the results of applying the GLM on these data in the section. Then in Sect. 4, we describe current available Hubble data from different observations and perform an MCMC parameter inference to obtain the best value of parameters as well as their uncertainties. We also apply the GLM method to the observational data and compare the results with those of the MCMC. Finally, we conclude and discuss the main points of our finding in Sect. 5.

2 Gaussian linear model

In this section, we briefly provide the basic formalism of the GLM. In this scenario, a database is modeled by a function which is linear in its parameters

$$f(x,\theta) = \sum \theta_j X^j(x), \tag{1}$$

where $X(x)$ is an arbitrary function of x and θ_js are the free parameters. Notice that the base functions can very well be a non-linear function of x. Assuming a n_{obs} dimension database as (x_i, y_i, τ_i), the likelihood function is given by

$$p(y|\theta) = \mathscr{L}_0 \exp\left[-\frac{1}{2}(\theta-\theta_0)^t L(\theta-\theta_0)\right] \tag{2}$$

where,

$$\mathscr{L}_0 = \frac{1}{(2\pi)^{n_{obs}/2}\Pi\tau_i}\exp\left[-\frac{1}{2}(b-A\theta_0)^t L(b-A\theta_0)\right], \tag{3}$$

and

$$F_{ij} = X^j(x_i),\ A = \frac{F_{ij}}{\tau_i},\ b = \frac{y_i}{\tau_i},\ L = A^t A,\ \theta_0 = L^{-1}A^t b. \tag{4}$$

Here the maximum likelihood occurs at θ_0 and L denotes the likelihood Fisher matrix.

In order to perform the Bayesian parameter inference, we need to define a prior on the free parameters. We consider a Gaussian prior as

$$p(\theta) = \frac{|\Sigma_{pri}|^{-1/2}}{(2\pi)^{n_{par}/2}}\exp\left[-\frac{1}{2}(\theta-\theta_{pri})^t \Sigma_{pri}^{-1}(\theta-\theta_{pri})\right], \tag{5}$$

where θ_{pri} (Σ_{pri}) is the mean (covariance matrix) of the prior and n_{par} denotes the number of free parameters. Using the Bays theorem, the posterior distribution is proportional to

$$p(\theta|y) \propto \exp\left[-\frac{1}{2}(\theta-\theta_{pos})^t \Sigma_{pos}^{-1}(\theta-\theta_{pos})\right], \tag{6}$$

where

$$\Sigma_{pos}^{-1} = \Sigma_{pri}^{-1} + L$$

and

$$\theta_{pos} = (\Sigma_{pri}^{-1} + L)^{-1}(\Sigma_{pri}^{-1}\theta_{pri} + L\theta_0).$$

.

In addition to the Bayesian parameter inference, the GLM provides the Bayesian evidence which is a key quantity in model comparison. The Bayesian evidence includes an integration over all parameters space and is given by

$$p(y) = \int d\theta p(\theta) p(\theta|y). \tag{7}$$

Since both the prior and likelihood are a multivariate Gaussian in the GLM, the integral has an analytical solution. The Bayesian evidence in the GLM is given by,

$$p(y) = \mathscr{L}_0 |\Sigma_{pri}|^{-1/2} |\Sigma_{pos}|^{1/2} \exp(D), \tag{8}$$

where

$$D = \frac{1}{2}[(\theta_{pri}^t \Sigma_{pri}^{-1} + \theta_0^t L)(\Sigma_{pri}^{-1} + L)^{-1}(\Sigma_{pri}^{-1}\theta_{pri} + L\theta_0) - (\theta_{pri}^t \Sigma_{pri}^{-1}\theta_{pri} + \theta_0^t L\theta_0)], \tag{9}$$

and $|\Sigma|$ denotes the determinant of Σ. In Addition, as we mentioned before, it is possible to have a solution in the case of the flat priors. To see more details refer to [30].

Table 1 The Jeffreys' scales for interpreting the Bayes factor

$\lvert \ln B_{01} \rvert$	Strength of evidence
< 1	Inconclusive
1.	Weak evidence
2.5	Moderate evidence
5	Strong evidence

Table 2 The Kass–Raftery scales for interpreting the Bayes factor

$\lvert \ln B_{01} \rvert$	Strength of evidence
0 to 1	Inconclusive
1 to 3	Positive evidence
3 to 5	Strong evidence
> 5	Very strong evidence

When comparing two models $\mathscr{M}_0$ and $\mathscr{M}_1$, using the Bayes theorem, it is straightforward to obtain,

$$\frac{p(\mathscr{M}_0|d)}{p(\mathscr{M}_1|d)} = B_{01}\frac{p(\mathscr{M}_0)}{p(\mathscr{M}_1)}, \tag{10}$$

where B_{01} is the Bayes factor. Usually, the prior on the models $p(\mathscr{M})$ is taken to be flat and so the Bayes factor is the key quantity in Bayesian model comparison. The value of Bayes factor should be interpreted by an empirically calibrated scale to compare given models. The Jeffreys' [33] and the Kass–Raftery scales [34] provides two well-known scales to interpret the Bayes factor. These two scales are presented in Tables 1 and 2.

Notice that these evidences are in favor of the model with larger evidence.

3 Simulated data and results

In order to apply the GLM in the cosmological context, we should have a linear model. As it has been shown in the following, there are a few simple models which are linear in their parameters. Considering the ΛCDM model, the Hubble parameter as a function of redshift can be written as

$$\begin{aligned} H^2(z) &= 100^2[\Omega_m h^2(1+z)^3 + h^2 - \Omega_m h^2] \\ &= 100^2[\Omega_m h^2((1+z)^3 - 1) + h^2], \end{aligned} \tag{11}$$

where $H_0 = 100h$ is the current expansion rate of the universe and Ω_m is the matter density parameter. Interestingly, the second format is linear in their parameters and can be consider as a GLM with

$$X^1(z) = (1+z)^3 - 1, \quad X^2(z) = 1$$

and free parameters

$$\theta_1 = \Omega_m h^2, \quad \theta_2 = h^2.$$

In addition to the ΛCDM, the wCDM with a fixed value of w, also can be written as a linear model.

$$H^2(z) = 100^2[\Omega_m h^2((1+z)^3 - (1+z)^{3(1+w)}) + h^2(1+z)^{3(1+w)}], \tag{12}$$

Notice that the above equation is not linear in w, but when the value of w is set to a constant, we can apply the GLM with

$$X^1(z) = (1+z)^3 - (1+z)^{3(1+w)}, \quad X^2(z) = (1+z)^{3(1+w)}$$

and free parameters

$$\theta_1 = \Omega_m h^2, \quad \theta_2 = h^2.$$

Where the w is not a free parameter in this case.

For the non-flat ΛCDM (NΛCDM) the Hubble parameter can be written as a linear model,

$$H^2(z) = 100^2[\Omega_m h^2((1+z)^3 - 1) + \Omega_k h^2((1+z)^2 - 1) + h^2], \tag{13}$$

In this case, the Ω_k is the curvature density parameter. These are linear models which we can use the GLM to find their free parameters as well as the Bayesian evidence.

To obtain the posterior distributions and the evidence, we need to define a prior on the free parameters. To avoid any possible prior bias, we consider a Gaussian wide prior on the free parameters. We use a multivariate Gaussian with mean and covariance matrix as

$$\theta_{pri} = (\Omega_m h^2 = 0.13, \Omega_k h^2 = 0., h^2 = 0.45) \tag{14}$$

$$\begin{bmatrix} 0.05 & 0 & 0 \\ 0 & 0.1 & 0 \\ 0 & 0 & 0.1 \end{bmatrix} \tag{15}$$

where the first, second and third row present covariance of the $\Omega_m h^2$, $\Omega_k h^2$ and h^2 respectively. We examine different mean and covariance matrix to check the robustness of our results. As long as the priors are wide enough, our results are the same and there is no prior bias.

3.1 ΛCDM and wCDM

In order to realize how precision and sampling rate of an expansion rate database affects the model comparison, we simulate the expansion rate data with different precision and use the GLM method to perform a model comparison. To compare the ΛCDM and wCDM, two sampling rates have been considered. In the first case, we simulate 100 data points in range $z \in (0, 3)$ with uncertainty $\sigma \in (0.5, 10\%)$ using the

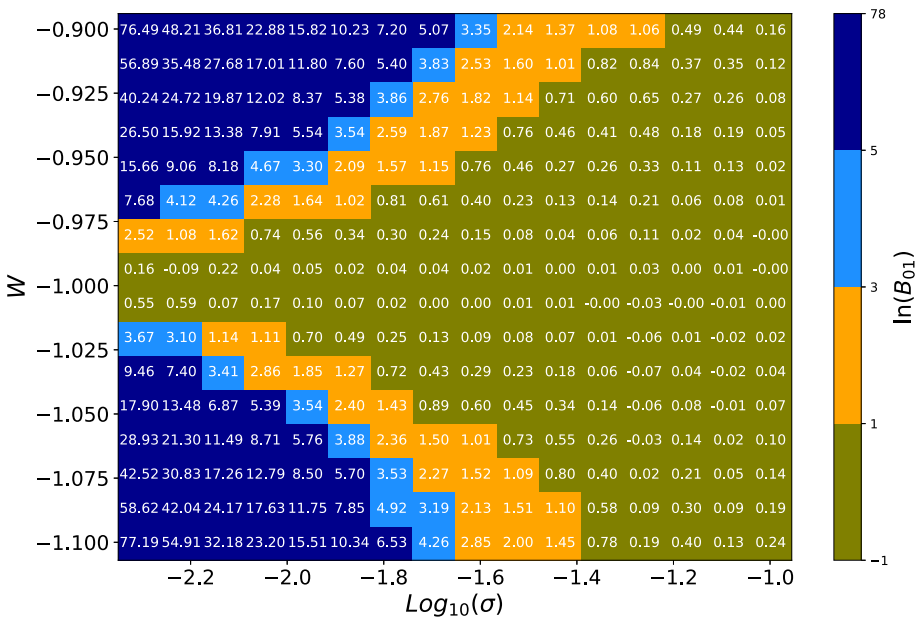

Fig. 1 The mean Bayes factor for the ΛCDM and wCDM using the first sampling strategy. Different colors show different criterion in Table 2

ΛCDM model. For the second sampling strategy, we simulate 50 data points in the redshift range $z \in (0, 2)$ and a similar uncertainty range as the first one. It is well known that the uncertainty changes at different redshift and so considering the same uncertainty for all redshifts is not a reliable choice. Since, in this work, we are going to investigate how Hubble data uncertainty affects discriminating a deviation in ΛCDM through Bayesian evidence, we consider the same uncertainty for all redshifts. To this aim, we consider the simulated data and compute the evidence for both ΛCDM and wCDM. In our analysis, the EoS, is selected in a range ($w \in -0.9, -1.1$). Moreover, we consider a Gaussian distribution for the uncertainty and so the data points are randomly generated at each simulation. Taking this into account, we have a distribution of the Bayes factor. In order to consider such a statistical fluctuation, we have generated 40 simulated data sets and compute the mean of Bayes factor. Notice that, we examine other values for the number of data sets and the results are quite the same by considering more data sets. The mean Bays factor $\ln B_{01} = \ln B_\Lambda - \ln B_w$ for two strategies, have been shown in Figs. 1 and 2 respectively. The value of Bays factor for each cell is shown as a numerical value on the cell.

From Fig. 1, it is clear that discriminating ΛCDM from wCDM with uncertainty larger than $10^{(-1.4)} \sim 4\%$ for a wide range of EoS is almost impossible. With $\sim 3\%$ uncertainty, we see a strong evidence only for $w \sim -0.9$ or $w \sim -1.1$, which is already disfavored by other observations. On the other hand, with $\sigma \leq 1\%$, the chance of discriminating increases significantly. For example with $\sigma = 0.5\%$, a 2% deviation in the EoS of dark energy ($w = 1.02$ or $w = 0.98$) could be detected with a strong evidence. Notice that, as we mentioned above, the base model for simulated data is the ΛCDM and the Bayes factor is computed for the ΛCDM and wCDM. Contrary, if we consider the wCDM as the base model for simulated data and compute the Bayes factor as $\ln B_{01} = \ln B_w - \ln B_\Lambda$, the results are the same. In this case, a positive Bayes factor indicates more evidence in favor of the wCDM.

In addition to the precision of each data point, the sampling rate of a database affects the model comparison. For a less cadence database, the results are presented in Fig. 2. Overall, the results are the same as the first sampling strategy but strength of the Bayes factor decreases. For example the extreme case in the first sampling strategy is $\ln B_{01} \sim 80$ for $\sigma = 0.5\%$ and $w = -0.9$, while considering the second strategy, the number decreases to $\ln B_{01} \sim 33$ which is around 60% less than the former.

3.2 ΛCDM and the non-flat ΛCDM

As we mentioned above, the NΛCDM can also be written in the form of a GLM. In this case, we follow similar strategies as previous one. The parameter $\Omega_k h^2$ is selected in the range $\Omega_k h^2 \in (-0.05, 0.05)$ to simulate data points. In this case, we simulate the Hubble data using NΛCDM and compute the evidence in both NΛCDM and ΛCDM. In Figs. 3 and 4 the mean Bayes factor (averaging over 40 databases) $\ln B_{01} = \ln B_N - \ln B_\Lambda$ have been shown for two sampling strategies. Here B_N indicates the evidence of the NΛCDM model.

Our results indicate that with $\sigma > 3\%$ there is no chance to discriminate a flat and non flat ΛCDM models. The evidence become more significant at both positive and negative curvature with smaller uncertainties. We see very strong evidence for $\Omega_k h^2 \sim 0.02$ with $\sigma < 1\%$ which is much higher for larger and smaller values of $\Omega_k h^2$. Furthermore, interestingly, we see a negative evidence for a high accuracy data $\sigma < 1\%$ when $\Omega_k h^2 \sim 0$. This is due to the Occam's

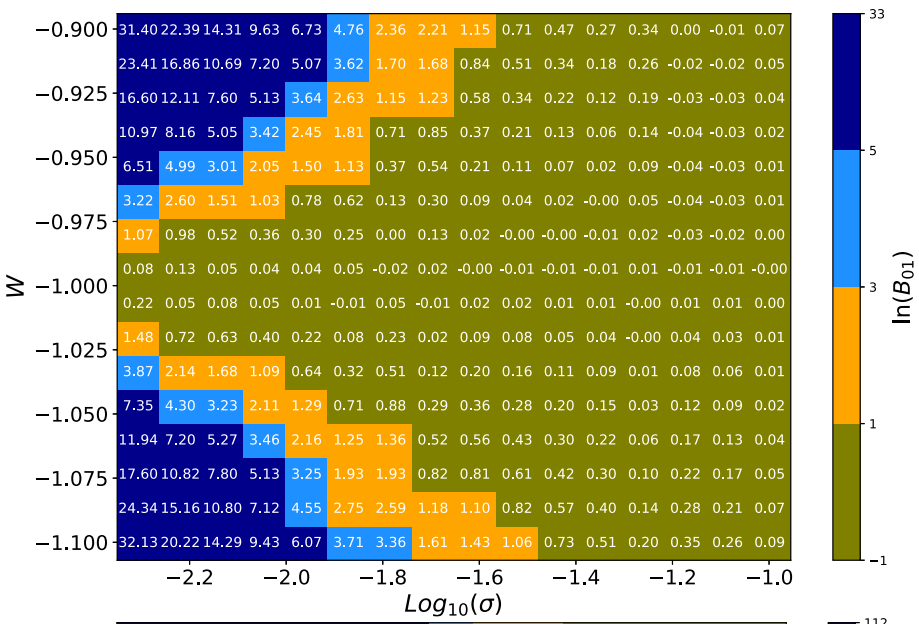

Fig. 2 The mean Bayes factor for the ΛCDM and wCDM using the second sampling strategy. Different colors show different criterion in Table 2

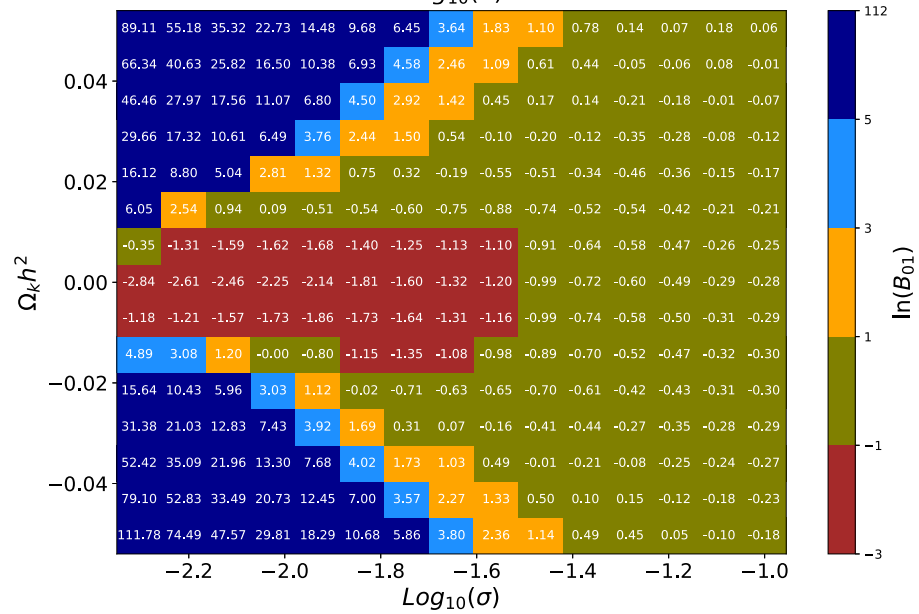

Fig. 3 The mean Bayes factor for the ΛCDM and NΛCDM using the first sampling strategy. Different colors show different criterion in Table 2

razor effect which favor a simpler model. The effect indicates that an extra free parameter, not being constrained significantly with the data, makes the evidence smaller compare to the model without that free parameter. In these cases, the Bayes factor favor the simpler model which is in our case the flat ΛCDM. Of course the constrain for $\Omega_k h^2$ is significantly improved for larger and smaller value of $\Omega_k h^2$ so the evidence become positive and the more complex model is favored.

The results for the second sampling strategy have been shown in Fig. 4. As the previous case, the strength of the evidence decreases for a less cadence sampling rate. In this case, the extreme case decreases around 75% in the second sampling rate.

4 Evidence for current available Hubble data

In this section, we apply the GLM approach on the current observational data. The expansion rate database in our analysis is a combination of the Hubble parameter measurement from cosmic chronometers and the BAO measurements. The database has been collected in [35]. The BAO data points have low uncertainty compare to the cosmic chronometer, in fact their uncertainties are in range (2−9)%. On the other hand, except two cosmic chronometers with uncertainty around 5%, other data points have uncertainties larger than 10%. According to our results, we do not expect to discriminate wCDM from the ΛCDM using these data set. In addition, it is worth noting that the cosmic chronometers data are not independent from each others and according to

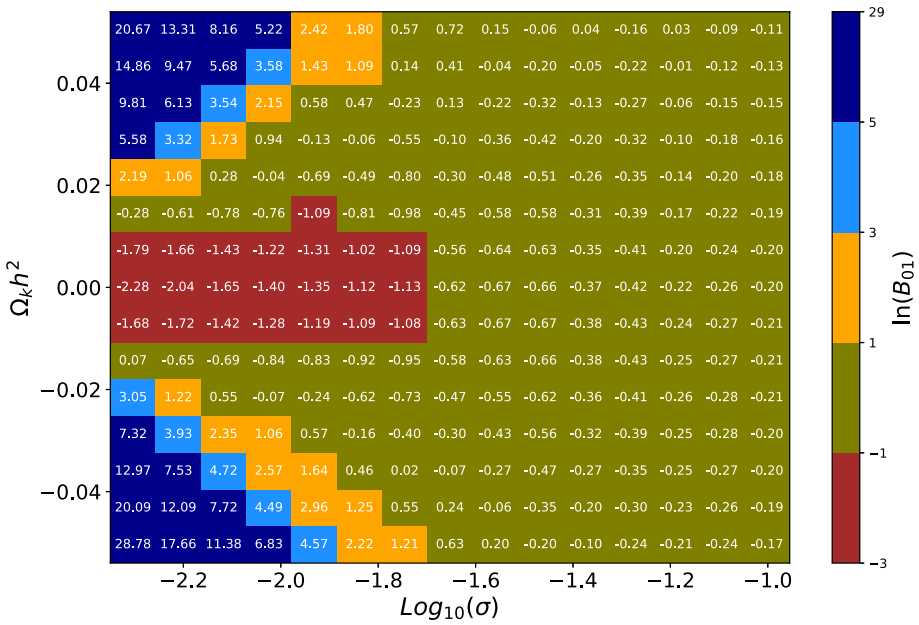

Fig. 4 The mean Bayes factor for the ΛCDM and NΛCDM using the second sampling strategy. Different colors show different criterion in Table 2

Table 3 The mean and uncertainty of parameters in ΛCDM and NΛCDM using MCMC method

Model/parameters	h^2	$\Omega_m h^2$	$\Omega_k h^2$
ΛCDM	0.518 ± 0.015	0.123 ± 0.005	–
NΛCDM	0.526 ± 0.018	0.135 ± 0.016	-0.034 ± 0.044

Table 4 The mean and uncertainty of parameters in ΛCDM and NΛCDM using the GLM method

Model/Parameters	h^2	$\Omega_m h^2$	$\Omega_k h^2$
ΛCDM	0.517 ± 0.015	0.121 ± 0.005	–
NΛCDM	0.526 ± 0.018	0.134 ± 0.016	-0.038 ± 0.044

[36], systematic uncertainty might add (2−5.5)% additional uncertainty. Since current cosmic chronometers data are not accurate enough to discriminate models, we do not consider the non-diagonal terms of the covariance matrix in this work.

In addition, the local H_0 measurement (the SHOES data) [5] has been added to the database. Considering the ΛCDM, wCDM and the non-flat ΛCDM, the results of MCMC analysis have been shown in the Table 3. To perform the MCMC analysis, we use the public python package *pymc3* [37]. In this analysis, we consider the wide Gaussian prior on the free parameters introduced in Sect. 3. The 1σ uncertainty of each parameters has been shown along with its mean value. These values are estimated from a sample of parameters generated in the MCMC algorithm.

Now, we use the database and apply the GLM formalism to obtain the MLE, mean and covariance of posterior as well as the evidence. The results have been presented in Table 4. As it is clear, the results from the GLM are quit in agreement with those of the MCMC. Notice that, in the case of GLM, we have an analytic posterior distribution for the free parameters and compute the mean and 1σ uncertainty directly from the distributions.

In our analysis, we find $\ln B_{01} = \ln B_\Lambda - \ln B_N = 0.43$ which indicates an inconclusive evidence for considered models. In fact, this result was expected because of the low precision observational data points. Notice that the most data points from cosmic chronometer have uncertainty larger than 10% but uncertainty of the expansion rate data from BAO is less than 10% and the uncertainty of the most precise one is $\sigma \sim 3.5\%$.

5 Conclusion

The landscape of cosmological models has drastically increased in recent years with the combined open problems of cosmological tensions and the internal consistency issues of gravitational models. In this work, we explore the GLM in the context of three cosmological models, namely ΛCDM, non-flat ΛCDM and the wCDM, in order to explore the question of precision requirements for specific data sets to discriminate these models. We wish to assess the data set precision needed to differentiate between each pair of these cosmological models.

Vanilla ΛCDM is our base model for considering any modification to the concordance model. Here, we compare ΛCDM together with wCDM where the equation of state parameter is allowed to be any value. These two model are central to modern cosmology and have Friedmann equations represented by Eqs. (11) and (13) respectively. In addition, we also consider ΛCDM with a possible non-flat component in Eq. (12). There have been recent suggestions in the litera-

ture that such a scenario may be preferable in the context of recent reporting by the Planck collaboration data [38].

The GLM approach presented here takes Friedmann equation components, and through a calculation resulting in the Bayes factor, can determine whether enough precision is present to differentiate between pairs of models. In Figs. 1 and 2 this is done for the ΛCDM and wCDM models where two sampling strategies are shown with very consistent results. Here, we find that indeed for an equation of state parameter that veers away from the ΛCDM value, the approach indicates a high confidence for differentiating these models. Specifically, we see a strong evidence in favor of the ΛCDM when the data simulated with uncertainty $\sigma \sim 0.5$ and the rival model is the wCDM with $w = -1.02$ or $w = -0.98$. Moreover, we show how different sampling rates affects the Bayes factor. The pattern of the results are almost the same for our two sampling strategies but the value of the Bayes factor is smaller in the case of the less cadence sampling.

In Figs. 3 and 4 we repeat the analysis for the ΛCDM and a non-flat ΛCDM setting. Our results indicate that it is impossible to discriminate these models with $\sigma > 3\%$ even if the $\Omega_k h^2$ is in the range $(-0.05, 0.05)$. The strength of the evidence become much more larger for $\Omega_k h^2$ not close to zero with uncertainty $\sigma < 3\%$. In addition, we see clear evidence of Occam's razor effect when the curvature density is close to zero.

Although the application of the GLM method is limited to a few cases, it provides a deep inside in understanding the discrimination of a deviation in the ΛCDM model through Bayesian evidence. To make this procedure as transparent as possible, we made a code for this analysis which is available for others to use and improve upon.[1]

Data Availability Statement This manuscript has no associated data or the data will not be deposited. [Authors' comment: In this study, we use public data that have been cited inside the paper. There is no new experimental data.]

Funded by SCOAP[3]. SCOAP[3] supports the goals of the International Year of Basic Sciences for Sustainable Development.

[1] https://github.com/Ahmadmehrabi/GLM.

References

1. A.G. Riess et al., Astron. J. **116**, 1009 (1998). https://doi.org/10.1086/300499
2. S. Perlmutter et al., Astrophys. J. **517**, 565 (1999). https://doi.org/10.1086/307221
3. N. Aghanim et al., Astron. Astrophys. **641**, A6 (2020). https://doi.org/10.1051/0004-6361/201833910
4. S. Alam et al., Phys. Rev. D **103**(8), 083533 (2021). https://doi.org/10.1103/PhysRevD.103.083533
5. A.G. Riess, S. Casertano, W. Yuan, L.M. Macri, D. Scolnic, Astrophys. J. **876**(1), 85 (2019). https://doi.org/10.3847/1538-4357/ab1422
6. E. Di Valentino et al., Astropart. Phys. **131**, 102606 (2021). https://doi.org/10.1016/j.astropartphys.2021.102606
7. E. Di Valentino et al., Astropart. Phys. **131**, 102605 (2021). https://doi.org/10.1016/j.astropartphys.2021.102605
8. A.G. Riess et al., Astrophys. J. Lett. **934**(1), L7 (2022). https://doi.org/10.3847/2041-8213/ac5c5b
9. S. Weinberg, Rev. Mod. Phys. **61**, 1 (1989). https://doi.org/10.1103/RevModPhys.61.1
10. C. Bengaly, Phys. Dark Univ. **35**, 100966 (2022). https://doi.org/10.1016/j.dark.2022.100966
11. T. Nadolny, R. Durrer, M. Kunz, H. Padmanabhan, JCAP **11**, 009 (2021). https://doi.org/10.1088/1475-7516/2021/11/009
12. E.J. Copeland, M. Sami, S. Tsujikawa, Int. J. Mod. Phys. D **15**, 1753 (2006). https://doi.org/10.1142/S021827180600942X
13. D. Benisty, D. Staicova, (2021). arXiv:2107.14129
14. D. Benisty, D. Staicova, Astron. Astrophys. **647**, A38 (2021). https://doi.org/10.1051/0004-6361/202039502
15. S. Vagnozzi, Phys. Rev. D **102**(2), 023518 (2020). https://doi.org/10.1103/PhysRevD.102.023518
16. T. Clifton, P.G. Ferreira, A. Padilla, C. Skordis, Phys. Rep. **513**, 1 (2012). https://doi.org/10.1016/j.physrep.2012.01.001
17. E.N. Saridakis et al., (2021). arXiv:2105.12582
18. S. Bahamonde, K.F. Dialektopoulos, C. Escamilla-Rivera, G. Farrugia, V. Gakis, M. Hendry, M. Hohmann, J.L. Said, J. Mifsud, E. Di Valentino (2021). arXiv:2106.13793
19. R. Alves Batista et al. (2021). arXiv:2110.10074
20. A. Addazi et al. Prog. Part. Nucl. Phys. **125**, 103948 (2022). https://doi.org/10.1016/j.ppnp.2022.103948
21. E. Di Valentino, O. Mena, S. Pan, L. Visinelli, W. Yang, A. Melchiorri, D.F. Mota, A.G. Riess, J. Silk, Class. Quantum Gravity **38**(15), 153001 (2021). https://doi.org/10.1088/1361-6382/ac086d
22. M. Vazirnia, A. Mehrabi, Phys. Rev. D **104**(12), 123530 (2021). https://doi.org/10.1103/PhysRevD.104.123530
23. A. Mehrabi, S. Basilakos, Eur. Phys. J. C **80**(7), 632 (2020). https://doi.org/10.1140/epjc/s10052-020-8221-2
24. A. Mehrabi et al., Mon. Not. R. Astron. Soc. **509**(1), 224 (2021). https://doi.org/10.1093/mnras/stab2915
25. E. Abdalla et al., JHEAp **34**, 49 (2022). https://doi.org/10.1016/j.jheap.2022.04.002
26. W.J. Handley, M.P. Hobson, A.N. Lasenby, Mon. Not. R. Astron. Soc. **450**(1), L61 (2015). https://doi.org/10.1093/mnrasl/slv047
27. J.S. Speagle, Mon. Not. R. Astron. Soc. **493**(3), 3132–3158 (2020). https://doi.org/10.1093/mnras/staa278
28. J. Alsing, W. Handley, Mon. Not. R. Astron. Soc. **505**(1), L95 (2021). https://doi.org/10.1093/mnrasl/slab057
29. R. Trotta, Mon. Not. R. Astron. Soc. **378**, 72 (2007). https://doi.org/10.1111/j.1365-2966.2007.11738.x
30. S. Nesseris, J. Garcia-Bellido, JCAP **08**, 036 (2013). https://doi.org/10.1088/1475-7516/2013/08/036
31. R.E. Keeley, A. Shafieloo, Mon. Not. Roy. Astron. Soc. **515**(1), 293–301 (2022). https://doi.org/10.1093/mnras/stac1851

32. H. Koo, R.E. Keeley, A. Shafieloo, B. L'Huillier, JCAP **03**(03), 047 (2022). https://doi.org/10.1088/1475-7516/2022/03/047
33. H. Jeffreys, *Theory of Probability*, 3rd edn. (Oxford University Press, Oxford, 1961)
34. R.E. Kass, A.E. Raftery, J. Am. Stat. Assoc. **90**(430), 773 (1995). https://doi.org/10.1080/01621459.1995.10476572. https://www.tandfonline.com/doi/abs/10.1080/01621459.1995.10476572
35. O. Farooq, F.R. Madiyar, S. Crandall, B. Ratra, Astrophys. J. **835**(1), 26 (2017). https://doi.org/10.3847/1538-4357/835/1/26
36. M. Moresco, R. Jimenez, L. Verde, A. Cimatti, L. Pozzetti, Astrophys. J. **898**(1), 82 (2020). https://doi.org/10.3847/1538-4357/ab9eb0
37. J. Salvatier, T.V. Wiecki, C. Fonnesbeck, PeerJ Comput. Sci. **2**, e55 (2016)
38. E. Di Valentino, A. Melchiorri, J. Silk, Nat. Astron. **4**(2), 196 (2019). https://doi.org/10.1038/s41550-019-0906-9